Electronic Supplementary Information (ESI)

An activatable fluorescent probe with an ultrafast response and large Stokes shift for live cell bioimaging of hypochlorous acid

Feng Liu, Ying Tang, Yongqing Kuang, Dan Pan, Xianjun Liu, Ru-Qin Yu*, Jian-Hui Jiang*

State Key Laboratory of Chemo/Biosensing and Chemometrics, College of Chemistry and Chemical Engineering, Hunan University, Changsha 410082, P. R. China

* Corresponding authors. E-mail: rqyu@hnu.edu.cn; jianhuijiang@hnu.edu.cn.

Tel.: 86-731-88822577; Fax: 86-731-88822872.

Table of Contents

1. Instrumentation

Mass spectra (MS) were performed using an LCQ Advantage ion trap mass spectrometer from Thermo Finnigan or Agilent 1100 HPLC/MSD spectrometer. ^{1}H NMR and ^{13}C NMR spectra spectra were recorded on a Bruker DRX-400 NMR spectrometer (Bruker) using tetramethylsilane (TMS) as an internal standard. UV-vis absorption spectra were plotted using a Shimadzu UV-2450 spectrophotometer with a wavelength interval of 2 nm. Fluorescence spectra were obtained on a HORIBA Fluoromax-4 spectrofluorometer (JobinYvon, Japan) with both excitation and emission slits set to 5.0 nm. The pH was verified using a Mettler-Toledo FE20 pH meter. The fluorescence imaging of cells was performed using a confocal laser scanning microscopy (Olympus, FV-1000).

2. Comparison of this method and other assays

Table S1. Comparison of this method and other assays

Methods	Materials				Linear range	Detection limit	Ref.
Colorimetric Method	N,N'-diethyl-p-phenylenediamine (DPD)				0-40 μM	-	1
Electrochemical Method	a commercial 2B pencil lead-based graphite sensor				0-6 ppm	0.303 μA ppm^{-1} cm^{-2}	2
Chemiluminescence Method	carbon nitride quantum dots (g-CNQDs)				0.02 -10 μM	0.01 μM	3
Fluorescent probe	Probes	$\lambda_{ex}/\lambda_{em}$ (nm)	Sensing moieties	Detection medium and [probe]	0-5 μM	25 nm	4
	AC-ClO	480/576	1,8-diamino naphthalene	PBS buffer (pH 10.0, 20 mM) and DMF (1/4, v/v), 5 μM			
	nanoprobe (MTPE-M)	340/498 -595	dicyanovinyl	PBS buffer solutions (pH 7.4, 10 mM, containing 1% DMSO and 1 mM CTAB) 10 μM	0-45 μM	0.47 μM	5
	HKOCl-3	490/527	2,6-dichlorophenol	PBS solution (10 mM, pH 7.4, DMF 0.1%) 10 μM	0-10 μM	0.33 nm	6
	BClO	480/505	pyrrole	PBS/EtOH (pH 7.4, 1:9); 1 μM	0-10 nm	0.56 nm	7
	HBP	480/508	heterocyclic hydrazone	PBS buffer-MeOH (v/v = 50/50, 50 mM PBS, pH7.4) 5 μM	1-8 μM	2.4 nm	8
	Probe 1b	464/505 540/585	diaminomaleonitrile	PBS buffer/DMF (pH 7.4, 8:2) 3 μM	0.9-90 μM	0.2 μM	9
	probe 1	450/556	oxime	H_2O:CH_3CN (99.5 : 0.5, v/v) buffered with HEPES (50 mM), pH = 7.4. 5 μM	0-25 μM	163 nM	10
	Flu-1	-/530	oxime	HEPES/DMSO (pH 7.05,1:9) 10 μM	-	-	11

	SeCy7	690/786	selenide	PBS buffer (pH 7.4) 30 μM	6-60 μM	310 nm	12
	CM1	405/480	selenide	PBS (pH=7.4) 4 μM	0-6.4 μM	10 nm	13
	HCSe	510/526	selenide	H_2O-CH_3CN (v/v = 99/1, 0.1 M PBS, pH 7.4) 10 μM	0-9 μM	7.98 nm	14
	Cou-Rho-HOCl	410/473-594	thiosemicarbazide	PBS/DMF (pH 7.4, 1:1) 5 μM	0.1-100 μM	52 nm	15
	RSTPP	553/580	thio-lactone	PBS (pH=7.4) 2.5 μM	0-35 μM	9 nM	16
	FBS	498/523	thio-lactone	KH_2PO_4 buffer (50 mM, pH 7.4) 2 μM	0-1.0 μM	200 nm	17
	PNIS	325/447	thione	PBS solution (50 mM, pH 7.4, DMF 0.2%) 2 μM	0-60 μM	210 nm	18
	Ptz-AO	475/540	thioether	H_2O 5 μM	0-25μM	2.7 nM	19
	Hypo-SiF	570/606	thioether	pH 7.4 phosphate buffer solution and 0.5% DMF 5 μM	-	-	20
	PZ–Py	400/562	thioether	PBS (pH 7.3, 10 mM, containing 0.05% DMSO) 5 μM	0-80 μM	17.9 nm	21
	Cy7-NpS	750/790	thioether	100 mM PBS, pH 7.40 10 μM	0-0.384 μM	0.62±0.09 μM	22
	TP-HOCl 1	375/500	1,3-oxathiolane	PBS/EtOH (1:1, PH 7.4) 5 μM	0-200 nm	16.6 nm	23
	HPBD	455/585	1,3-oxathiolane	PBS buffer-CH_3CN (v/v=4/1, 20 mM PBS, pH 7.4) 10 μM	0-40 μM	50 nm	This work

References

1 L. Moberg and B. Karlberg, Anal. Chim. Acta., 2000, **407**, 127-133.
2 S. Pan, M. J. Deen, R. Ghosh, Anal. Chem., 2015, **87**, 10734-10737.
3 Y. R. Tang, Y. Y. Su, N. Yang, L. C. Zhang, Y. Lv, Anal. Chem., 2014, **86**, 4528-4535.
4 J. L. Fan, H.Y. Mu, H. Zhu, J. Y. Wang, X. J, Peng., *Analyst*, 2015, **140**, 4594-4598.
5 Y. Huang, P. S. Zhang, M. Gao, F. Zeng, A. J. Qin, S.Z. Wu and B. Z. Tang, *Chem. Commun*., 2016, **52**, 7288-7291.
6 J. J. Hu, N.-K. Wong, M. Y. Lu, X. M. Chen, S. Ye, A. Q. Zhao, P. Gao, R. Y.-T. Kao, J. G. Shen and D. Yang, *Chem. Sci*., 2016, **7**, 2094-2099.
7 H. Zhu, J. L. Fan, J. Y. Wang, H. Y. Mu and X. J. Peng, *J. Am. Chem. Soc*., 2014, **136**, 12820-12823.
8 W.-C.Chen, P. Venkatesan, S.-P. Wu, *Anal. Chim. Acta*., 2015, **882**, 68-75.
9 L. Yuan, W. Y. Lin, J. Z. Song and Y. T. Yang, *Chem. Commun*., 2011, **47**, 12691-12693.
10 S. I. Reja, V. Bhalla, A. Sharma, G. Kaur and M. K, *Chem. Commun*., 2014, **50**, 11911-11914.
11 X. H. Cheng, H. Z. Jia, T. Long, J. Feng, J. G. Qin and Z. Li, *Chem. Commun*., 2011, **47**, 11978-11980.
12 G. H. Cheng, J. L. Fan, W. Sun, J. F. Cao, C. Hua and X. J. Peng, *Chem. Commun*., 2014, **50**, 1018-1020.
13 G. P. Li, D. J. Zhu, Q. Liu, L. Xue and H. Jiang, *Org. Lett*., 2013, **15**, 2002-2005.
14 S. R. Liu and S. P. Wu, *Org. Lett*., 2013, **15**, 878-881.
15 L. Yuan, W. Y. Lin, Y. N. Xie, B. Chen and J. Z. Song, *Chem. Eur. J*., 2012, **18**, 2700-2706.
16 Q. L. Xu, K.-A. Lee, S. Y. Lee, K. M. Lee, W.-J. Lee, and J. Y. Yoon, *J. Am. Chem. Soc*., 2013, **135**, 9944-9949.
17 Q. L. Xu, C. H. Heo, J. A. Kim, H. S. Lee, Y.Hu, D. Y. Kim, *Anal. Chem*., 2016, **88**, 6615-6620.
18 J. Zhou, L. H. Li, W. Shi, X. H. Gao, X. H. Li and H. M. Ma, *Chem. Sci*., 2015, **6**, 4884-4888.
19 L. J. Liang, C. Liu, X. J. Jiao, L.C. Zhao and X. S. Zeng, *Chem. Commun*., 2016, **52**, 7982-7985.
20 Q. A. Best, N. Sattenapally, D. J. Dyer, C. N. Scott, and M. E. McCarroll, *J. Am. Chem. Soc*., 2013, **135**, 13365-13370.
21 H. D. Xiao, K. Xin, H.F. Dou, G. Yin, Y. W. Quana and R. Y. Wang, *Chem. Commun*., 2015, **51**, 1442-1445.
22 F. S. Tian, Y.Jia, Y.N. Zhang , W. Song , G. J. Zhao, Z. J. Qu, C.Y. Li, Y. H. Chen, P. Li, *Biosensors and Bioelectronics*, 2016, **86**, 68-74.
23 L. Yuan, L. Wang, B. K.Agrawalla, S.-J. Park, H. Zhu, B. Sivaraman, J. J. Peng, Q.-H. Xu and Y.-T. Chang, *J. Am. Chem. Soc*., 2015, **137**, 5930−5938.
24 This workccc

3. Structure characterizations of **HPBD**, **HPBD-1**, **HPBD-2**

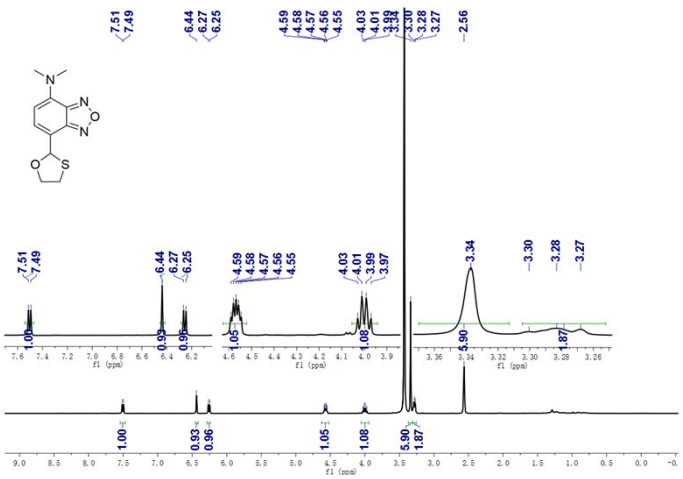

Fig. S1. ^{1}H NMR spectrum of **HPBD** in d_6-DMSO.

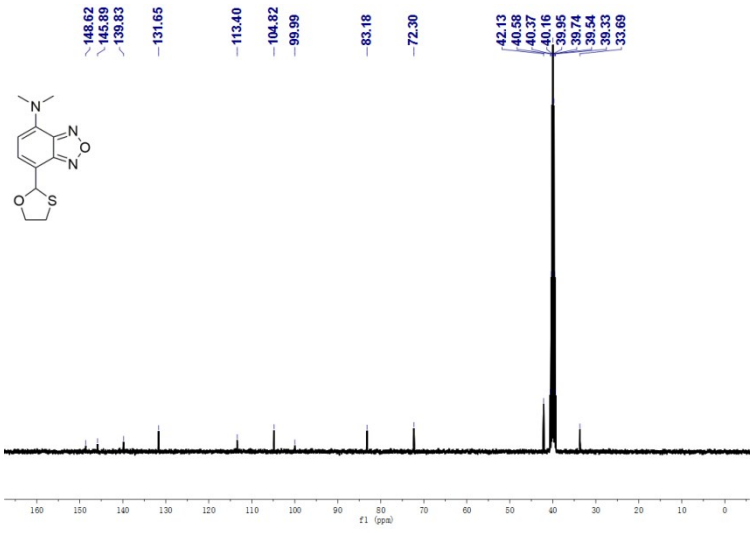

Fig. S2. ^{13}C NMR spectrum of **HPBD** in d_6-DMSO.

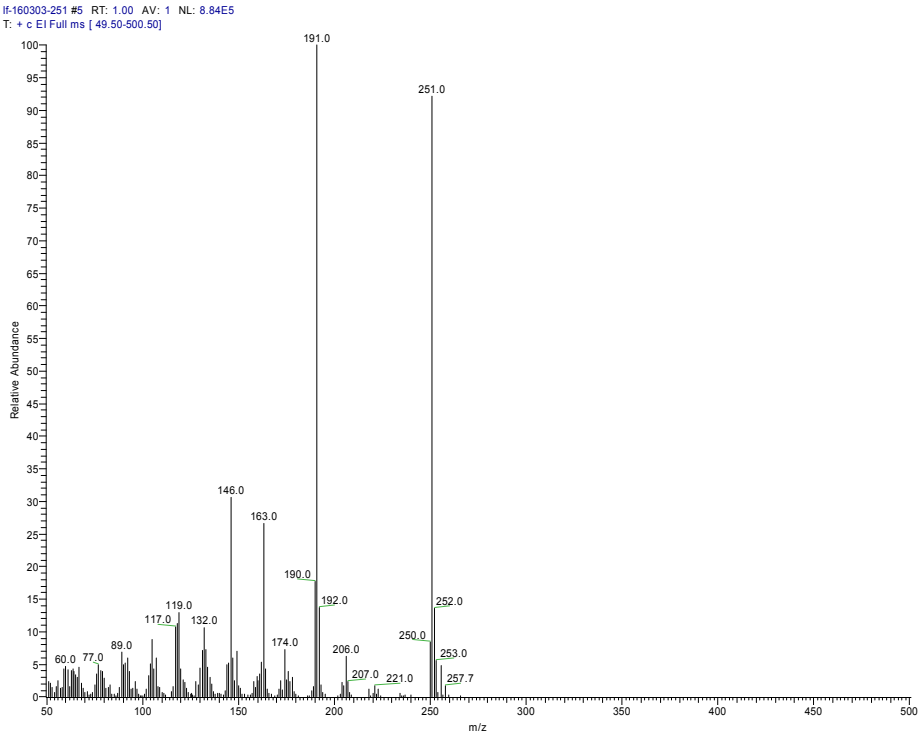

Fig.S3. EI spectrum of **HPBD** in Methanol.

File : D:\Xcalibur\data\lf-160303-251-hr-av2.RAW
Full ms [239.500 - 258.500] - Range: 239.500 - 258.500
Scan No. 1 of 1

Mass	Relative Intensity	Theoretical Mass	Delta [ppm]	Delta [mmu]	Composition
251.0725	100.0	251.0723	0.9	0.2	$C_{11}H_{13}O_2N_3S_1$
		251.0689	14.3	3.6	$C_{14}H_9O_2N_3$
		251.0815	-35.8	-9.0	$C_{15}H_{11}O_2N_2$
		251.0849	-49.2	-12.4	$C_{12}H_{15}O_2N_2S_1$
		251.0525	79.7	20.0	$C_{16}H_{11}O_1S_1$

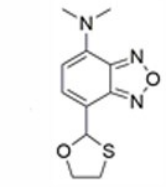

Fig. S4. HRMS (EI) spectrum of **HPBD** in Methanol.

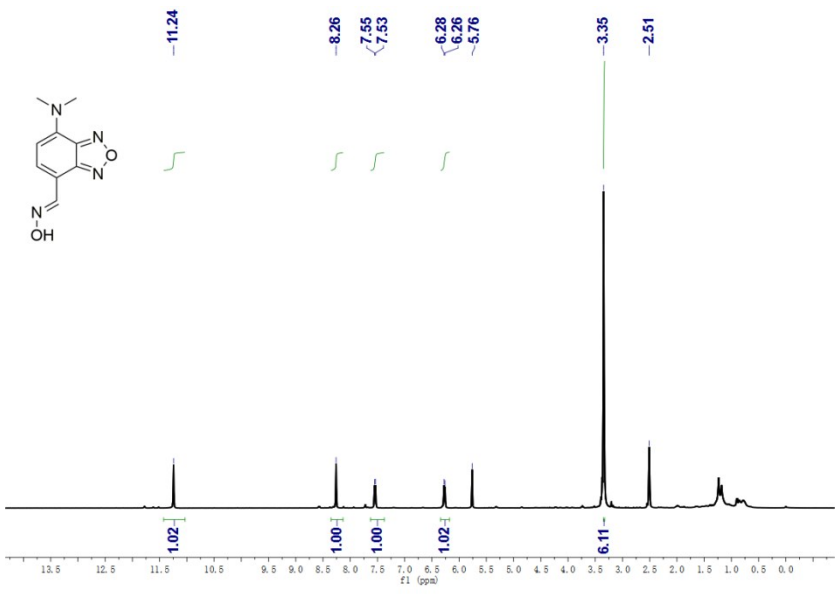

Fig.S5. ^{1}H NMR spectrum of **HPBD-1** in d_6-DMSO.

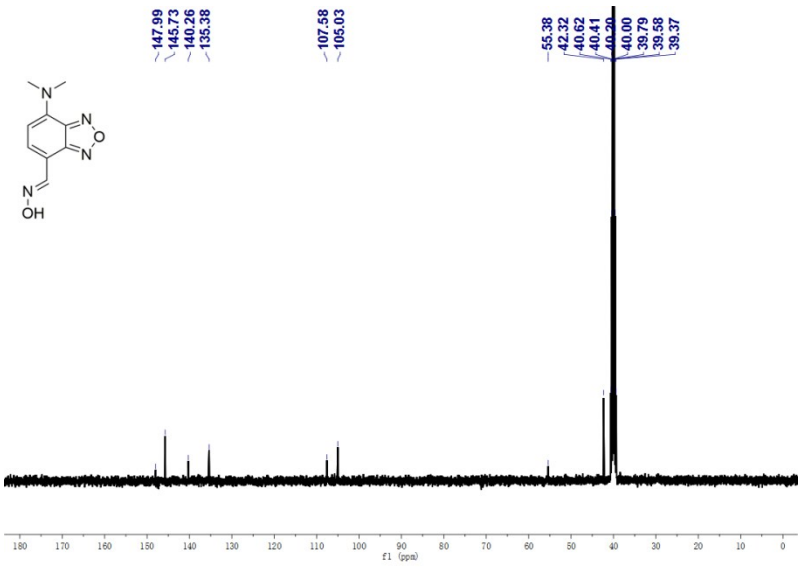

Fig. S6. ^{13}**C** NMR spectrum of **HPBD-1** in d_6-DMSO.

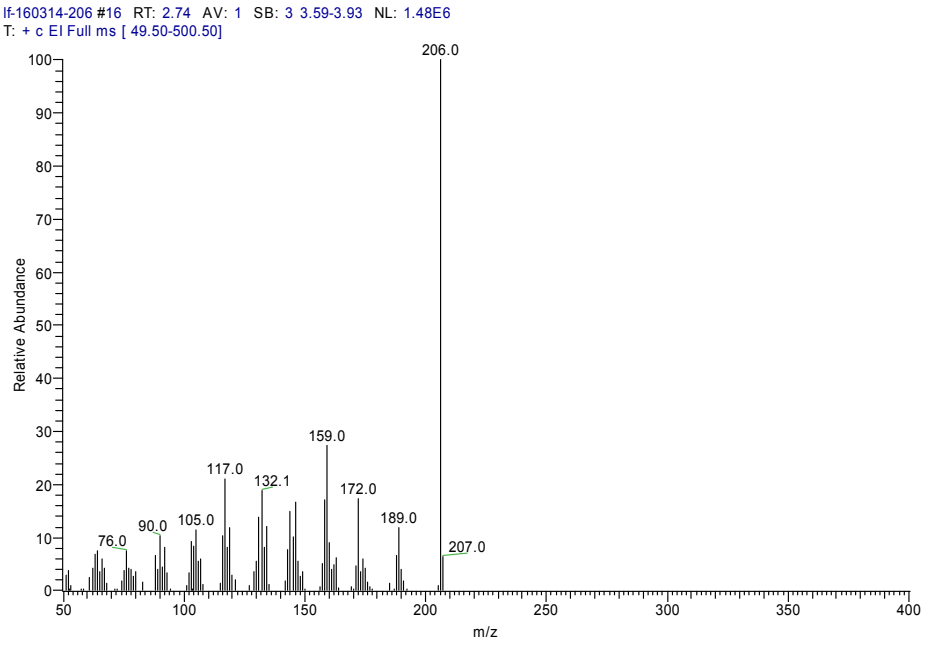

Fig.S7. EI spectrum of **HPBD-1** in Methanol.

File : D:\Xcalibur\data\lf-160315-206-hr-av2.RAW
Full ms [201.500 - 222.500] - Range: 201.500 - 222.500
Scan No. 1 of 1

Mass	Relative Intensity	Theoretical Mass	Delta [ppm]	Delta [mmu]	Composition
206.0806	103.8	206.0798	3.9	0.8	$C_9 H_{10} O_2 N_4$
		206.0838	-15.6	-3.2	$C_{14} H_{10} N_2$
		206.0726	38.9	8.0	$C_{15} H_{10} O_1$
		206.0713	45.4	9.4	$C_{13} H_8 N_3$
		206.0924	-57.1	-11.8	$C_{10} H_{12} O_2 N_3$

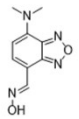

Fig.S8. HRMS (EI) spectrum of **HPBD-1** in Methanol.

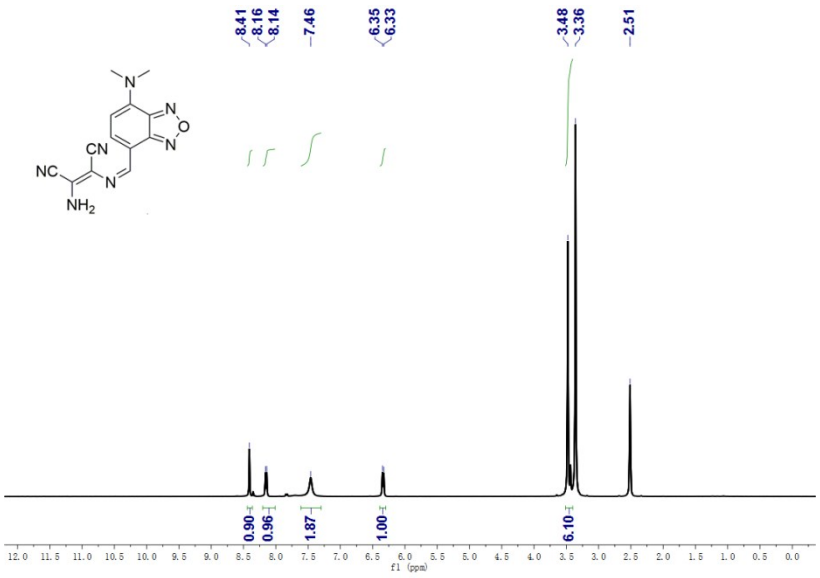

Fig.S9. ^{1}H NMR spectrum of **HPBD-2** in d_6-DMSO.

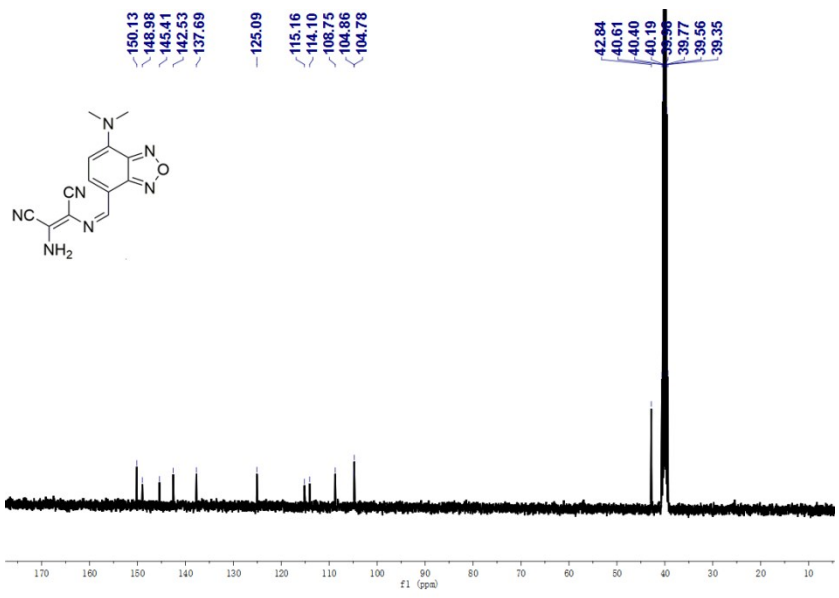

Fig. S10. ^{13}**C** NMR spectrum of **HPBD-2** in d_6-DMSO.

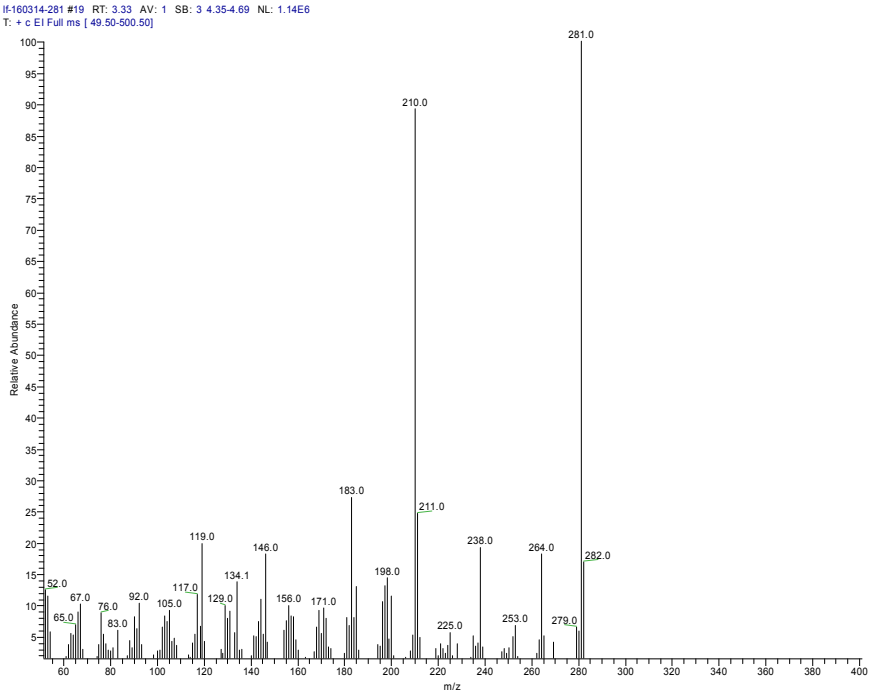

Fig.S11. EI spectrum of **HPBD-2** in Methanol.

File : D:\Xcalibur\data\lf-160315-281-hr-av2.RAW
Full ms [265.500 - 296.500] - Range: 265.500 - 296.500
Scan No. 1 of 1

Mass	Relative Intensity	Theoretical Mass	Delta [ppm]	Delta [mmu]	Composition
281.1014	100.0	281.1020	-2.0	-0.6	$C_{13}H_{11}O_1N_7$
		281.0961	18.9	5.3	$C_{21}H_{13}O_1$
		281.1073	-21.1	-5.9	$C_{20}H_{13}N_2$
		281.0947	23.6	6.6	$C_{19}H_{11}N_3$
		281.1145	-46.8	-13.1	$C_{14}H_{13}O_1N_6$

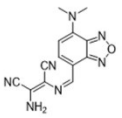

Fig.S12. HRMS (EI) spectrum of **HPBD-2** in Methanol.

4. Detection limit and linear range of **HPBD** for HOCl detection.

The spectrum of free **HPBD** (10 μM) was collected for 10 times to determine the background noise σ. Then the solution was treated with various concentration of HOCl from 0-40 μM. A linear regression curve was then fitted according to the emission intensity at 585 nm in the range of 0-40 μM. As exhibited in Fig.S13, **HPBD** can quantitatively detect HOCl in the range from 0 to 40 μM with good linearity (R^2 = 0.99604).

Another linear regression curve was then fitted according to the data in the range of HOCl from 0 to 4 μM, and the slope of the curve was obtained (Fig. S14). The detection limit (3σ/slope) was then determined to be 50 nM.

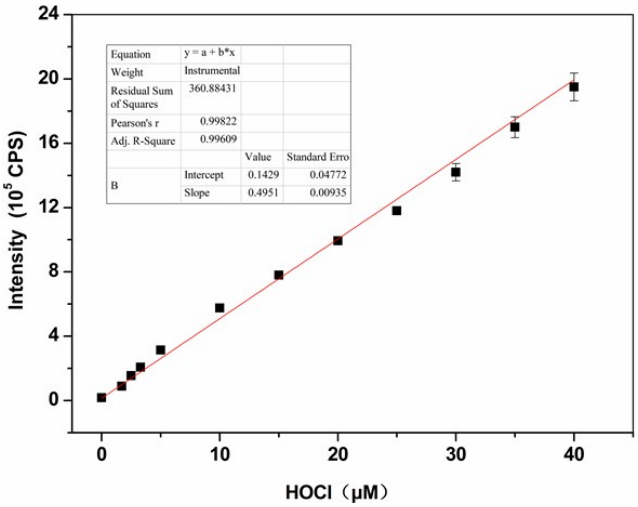

Fig. S13. The titration curve plotted with the fluorescnece intensity of **HPBD** (10 μM) at 585 nm as a function of HOCl concentration in range of 0-40 μM. λ_{ex}= 455 nm.

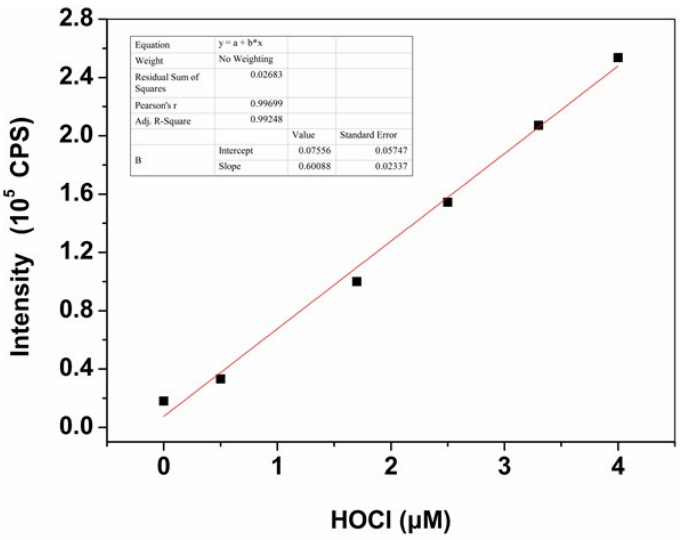

Fig. S14 The titration curve plotted with the fluorescnece intensity of **HPBD** (10 μM) at 585 nm as a function of HOCl concentration in range of 0-4 μM. λ_{ex}= 455 nm.

5. Colorimetric response of **HPBD** to various ROS and RNS

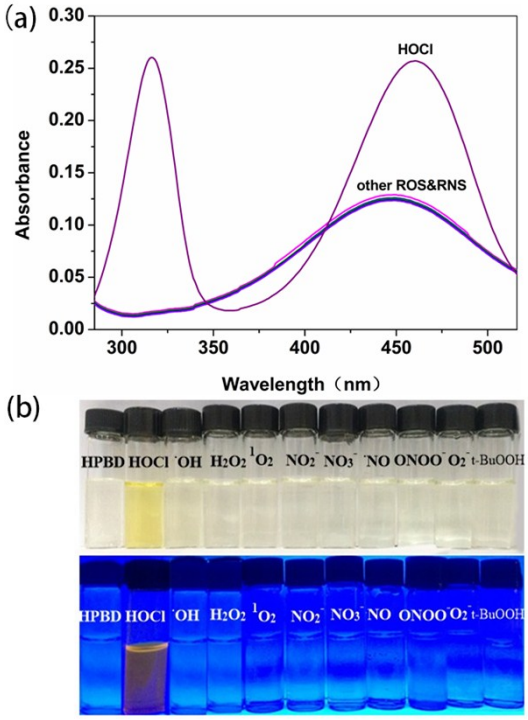

Fig.S15 (a) Absorption spectra of **HPBD** (10 μM) upon adding various ROS and RNS (40 μM) in a PBS buffer-CH_3CN(*v/v=4/1*, 20 mM PBS, pH 7.4). (b) Colorimetric (upper row) and fluorometric (lower row, irradiated at 365 nm) photographs of **HPBD** (25 μM) in a PBS buffer-CH_3CN (*v/v=4/1*, 20 mM PBS, pH 7.4). Left to right: **HPBD**, HOCl, ·OH, H_2O_2,$^1O_2$, NO_2^-, NO_3^-, NO, $ONOO^-$, O_2^- and t-BuOOH.

6. Sensing mechanism study

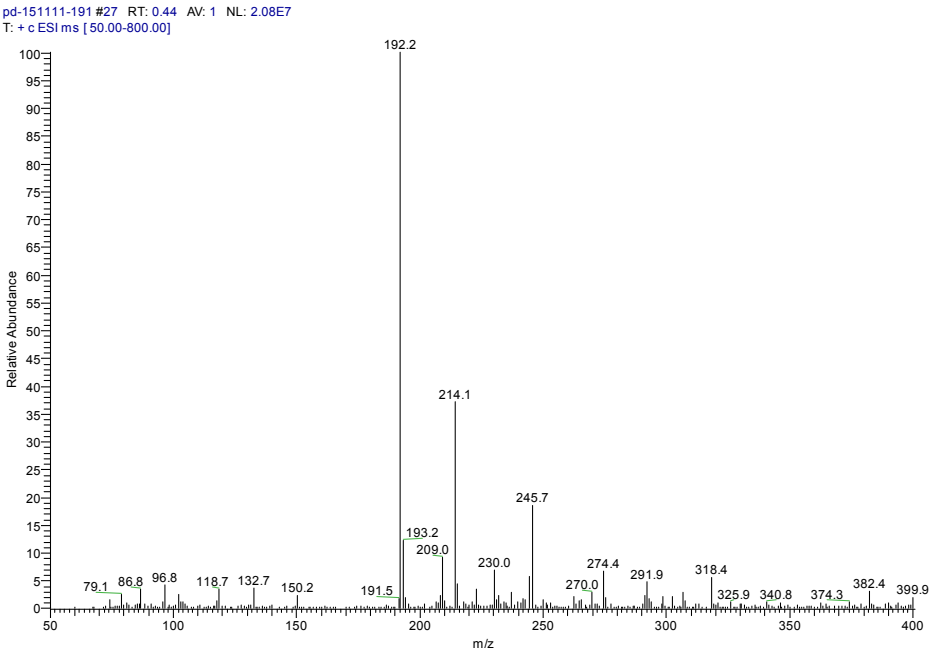

Fig.S16. ESI-MS spectrum of **HPBD**/HOCl mixture.

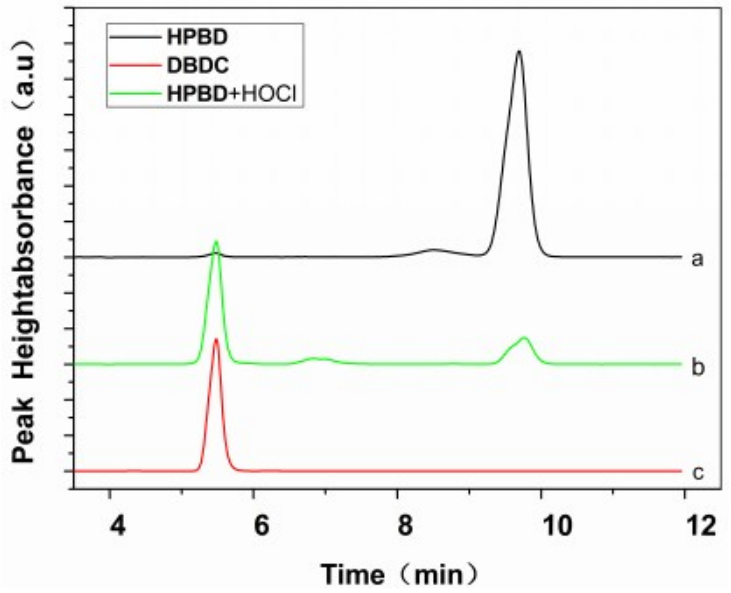

Fig.S17. Mechanistic study of probe reacting with HOCl and indentification of adduct using HPLC method. (a) 100 μM probe **HPBD**; (b) 100 μM **DBDC**; (c) the reaction products of 100 μM probe with HOCl. Detection: UV-vis (398 nm) detector. Flow rate: 1mL/min. T: 20 °C. Injection volume: 100 μL. Mobile phase: methanol/water=80/20 (*v/v*).

7. MTT assay

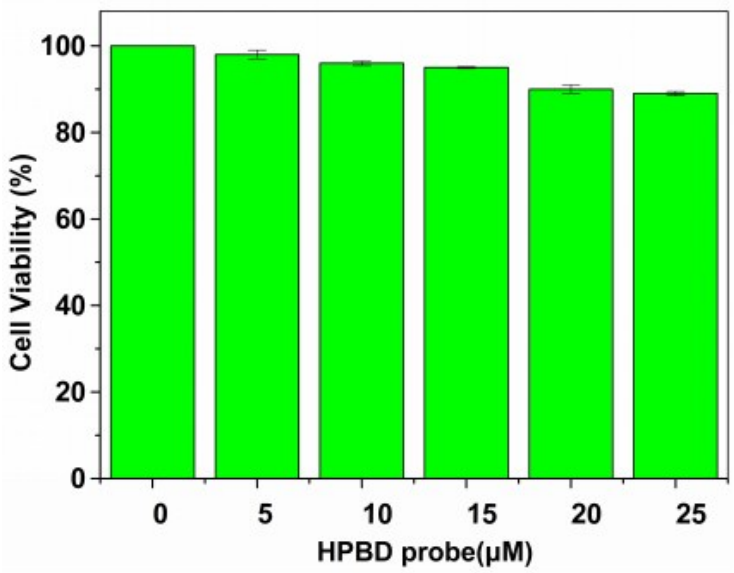

Fig. S18. Cytotoxicity assay of RAW 264.7 cells were treated in the presence of HPBD (0-25 μM) incubated for 24 h.